PRAMANA — journal of physics

Vol. 80, No. 3
March 2013
pp. 507–517

Generation of uniform atmospheric pressure argon glow plasma by dielectric barrier discharge

RAJU BHAI TYATA[1,2], DEEPAK PRASAD SUBEDI[1,*], RAJENDRA SHRESTHA[1] and CHIOW SAN WONG[3]

[1]Department of Natural Science, Kathmandu University, Dhulikhel, Nepal
[2]Department of Electrical Engineering, Khwopa College of Engineering, Libali-2, Bhaktapur, Nepal
[3]Plasma Technology Research Centre, Physics Department, University of Malaya, 50603 Kuala Lumpur, Malaysia
*Corresponding author. E-mail: deepaksubedi2001@yahoo.com

MS received 13 March 2012; revised 8 September 2012; accepted 18 September 2012

Abstract. In this paper, atmospheric pressure glow discharges (APGD) in argon generated in parallel plate dielectric barrier discharge system is investigated by means of electrical and optical measurements. Using a high voltage (0–20 kV) power supply operating at 10–30 kHz, homogeneous and steady APGD has been observed between the electrodes with gap spacing from 0.5 mm to 2 mm and with a dielectric barrier of thickness 2 mm while argon gas is fed at a controlled flow rate of 1 l/min. The electron temperature and electron density of the plasma are determined by means of optical emission spectroscopy. Our results show that the electron density of the discharge obtained is of the order of 10^{16} cm^{-3} while the electron temperature is estimated to be 0.65 eV. The important result is that electron density determined from the line intensity ratio method and stark broadening method are in very good agreement. The Lissajous figure is used to estimate the energy deposited to the glow discharge. It is found that the energy deposited to the discharge is in the range of 20 to 25 μJ with a discharge voltage of 1.85 kV. The energy deposited to the discharge is observed to be higher at smaller gas spacing. The glow discharge plasma is tested to be effective in reducing the hydrophobicity of polyethylene film significantly.

Keywords. Atmospheric pressure glow discharge; argon glow discharge; electron density; hydrophobicity

PACS No. 52

1. Introduction

Dielectric barrier discharge (DBD) and APGD are the subjects of research for the last few decades due to their wide range of potential applications in industry and medicine as well as in remediation of the environment and water treatment [1–6]. The interest

in these atmospheric pressure plasmas have been emphasized in practical applications because it minimizes the need for vacuum systems and enables the treatment of materials continuously [7]. The main advantage of APGD over filamentary DBD is that it offers a uniform plasma treatment which is necessary for the deposition of homogeneous thin film and uniform surface treatment [2,3,7].

In general, a stable glow discharge is easily achieved in low pressure of less than few mbar [8,9]. Most atmospheric pressure DBDs reported are filamentary and APGD is likely to be unstable and it tends to change to a filamentary discharge. The transition of atmospheric pressure discharge from glow to filamentary is strongly dependent on the type of gas used, the material of the dielectric, the structure of the discharge electrode, the frequency of the applied power source, the electrode spacing and the humidity of the gas [10,11].

However, several authors [12–15] have demonstrated the possibility of obtaining stable glow discharge at atmospheric pressure using a source frequency above 1 kHz, inserting dielectric plates between two metal electrodes and using He, Ne, Ar gases. The discharge is characterized by one single current pulse per half period of about 10 ns to 100 μs duration and a current of amplitude 10 mA to several amperes [16,17].

In this paper, we report the generation of argon APGD by DBD and its electrical and optical characterization. The application of the discharge for the surface modification of polyethylene (PE) to improve the hydrophilicity property has also been demonstrated.

2. Experimental set-up

The schematic diagram of the experimental arrangement used to study the APGD is shown in figure 1. The discharge is generated between two symmetric parallel electrodes. The electrodes are made of brass with smooth surface. They have 50 mm diameter and 10 mm thickness. The lower electrode is fixed and the upper one is movable with a pitch of 0.5 mm. Glass plate of 2 mm thickness is used as the dielectric. A high voltage AC power

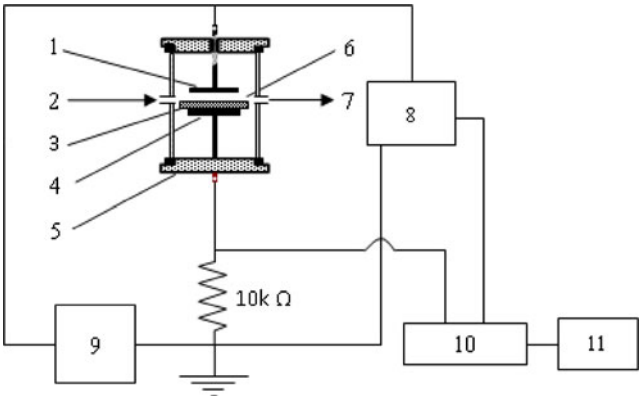

Figure 1. Schematic diagram of the experimental set-up. 1 – Electrode, 2 – gas inlet, 3 – dielectric, 4 – grounded electrode, 5 – bottom flange, 6 – discharge gap, 7 – gas outlet, 8 – HV probe, 9 – HV power supply, 10 – digital oscilloscope, 11 – PC.

supply is used and the applied voltage is in the range of 1–2 kV at a frequency of 30 kHz. The gap between the electrodes can be varied from 0.5 mm to 2 mm and Ar is fed at a flow rate of 1 l/min. A high voltage probe is used to measure the voltage applied across the electrodes while the discharge current is measured by using a shunt resistor at the earth side of the discharge tube. The signals are recorded using a Tektronix TDS2002 digital oscilloscope.

The experiments are carried out for gap spacing of 0.5 mm, 1 mm and 2 mm. The optical emission spectra in the range 190–800 nm are recorded by a HORIBA Jobin Yvon UV-VIS Spectrometer. Its focal length is 140 nm and grating per mm is 1200. Typical resolution with 100 μm core fibre is 2.3 nm and is connected with SMA connector.

Surface treatment of PE film of the commercial variety having 20–30 g/m^2 surface density has been carried out. The films are washed in ultrasonic bath with isopropyl alcohol for 10 min and then dried in air. The effect of the treatment time on the surface property of the sample is investigated by measuring the contact angle of the untreated and plasma-treated PE with water.

3. Results and discussion

3.1 *Electrical characterization*

Figure 2a shows the current and voltage waveforms of the discharge produced with 0.5 mm gap spacing. The corresponding image of the discharge is shown in figure 2b. The current waveform shows a displacement current with an amplitude of nearly 1.2 mA which leads the voltage indicating the capacitive nature of the DBD system. With low applied voltage, the current waveform is found to have many spikes representing the existence of filamentary discharge. The applied voltage is gradually increased upto 1.85 kV. The current waveform then becomes free of clustered filaments and there is only one spike in each half-cycle of the current waveform. The appearance of the single current spike per half-cycle is in fact an indication of transition from filamentary to glow discharge. In

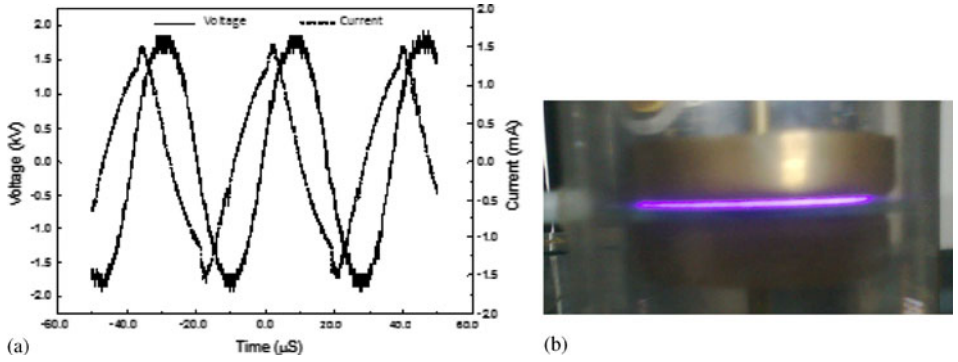

Figure 2. **(a)** Voltage and current waveforms of the APGD produced with a power supply operated at 26.5 kHz, gap spacing = 0.5 mm, thickness of the dielectric (glass) = 2 mm. **(b)** Photograph of the discharge.

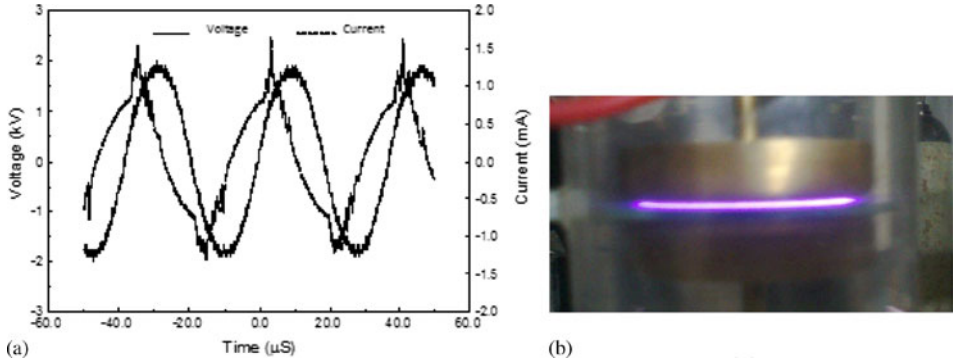

Figure 3. **(a)** Voltage and current waveforms of the APGD produced with a power supply operated at 26.5 kHz, gap spacing = 1 mm, thickness of the dielectric (glass) = 2 mm. **(b)** Photograph of the discharge.

this experiment, the voltage of AC power supply applied to the electrodes is increased gradually in the presence of Ar flow rate of 1 l/min. For a gap of 0.5 mm, the discharge is turned on when the voltage is increased to 0.53 kV. The peak current is 1.5 mA.

In the case of 1 mm gap as shown in figure 3a, 0.85 kV is required to ignite the discharge while the peak current in this case is 1.6 mA. Similarly, in the case of 2 mm gap as shown in figure 4a, 1.14 kV is required to turn on the discharge and the discharge current reaches a maximum of 2.0 mA. Figures 3b and 4b indicate the corresponding images of discharge in 1 mm and 2 mm gap respectively.

The breakdown voltage and the corresponding current during the negative half-cycle seem to be different from those at positive half-cycle. For 0.5 mm gap, the negative cycle gives higher peak discharge current but for 1 mm and 2 mm gaps, the peak discharge current at negative cycle is lower than that at positive cycle. It is important to

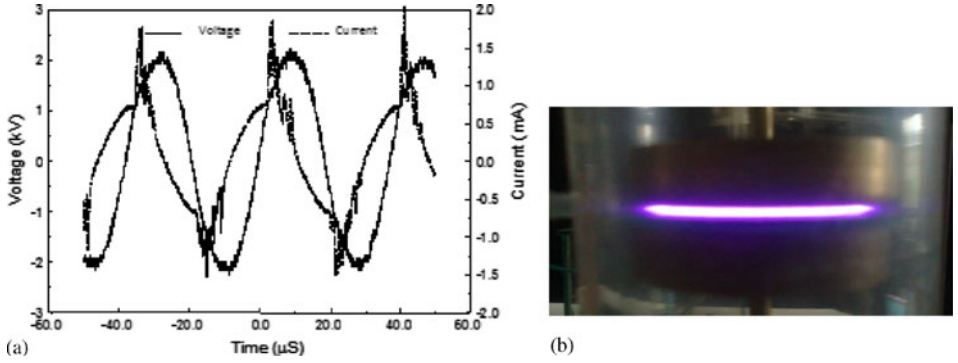

Figure 4. **(a)** Voltage and current waveforms of the APGD produced with power supply operated at 26.5 kHz, gap spacing = 2 mm, thickness of the dielectric (glass) = 2 mm. **(b)** Photograph of the discharge.

note that the change in current waveform is also due to the change in capacitance of the discharge system while changing the gap width.

3.2 *Determination of electron temperature and electron density by optical emission spectroscopy*

Figure 5 shows the optical emission spectra of the discharge produced between the electrodes with a gap of 2 mm. Four suitable lines (two belong to the neutral atom ArI and the other two belong to the first ionized specie ArII) have been chosen. Spectroscopic data for the four lines, $\lambda_{n1} = 696.54$ nm ($a_1 \rightarrow b_1$), $\lambda_{n2} = 751.034$ nm ($a_2 \rightarrow b_2$), $\lambda_{+1} = 314.13$ nm ($c_1 \rightarrow d_1$) and $\lambda_{+2} = 378.75$ nm ($c_2 \rightarrow d_2$) consist of the transition levels, A, g and E which are taken from NIST atomic spectra database.

The method we adopt here to determine the electron temperature of the APGD plasma involves taking line intensity ratio [19] for two pairs of lines as given by eqs (1) and (2).

$$R_1 = \frac{I_{+1}}{I_{n1}} = \frac{2}{n_e}\frac{\lambda_{n1}A_{+1}g_{c1}}{\lambda_{+1}A_{n1}g_{a1}}\left[\frac{2\pi m_e kT_e}{h^2}\right]^{3/2} e^{-(E_{a1}-E_{c1}+E_i)/kT_e}, \tag{1}$$

$$R_2 = \frac{I_{+2}}{I_{n2}} = \frac{2}{n_e}\frac{\lambda_{n2}A_{+2}g_{c2}}{\lambda_{+2}A_{n2}g_{a2}}\left[\frac{2\pi m_e kT_e}{h^2}\right]^{3/2} e^{-(E_{a2}-E_{c2}+E_i)/kT_e}. \tag{2}$$

By taking the ratio of R_1 and R_2 we then obtain the expression:

$$\frac{R_1}{R_2} = \frac{I_{+1}/I_{n1}}{I_{+2}/I_{n2}}$$

$$= \left(\frac{A_{+1}}{A_{n1}}\right)\left(\frac{g_{c1}}{g_{a1}}\right)\left(\frac{\lambda_{n1}}{\lambda_{+1}}\right)\left(\frac{A_{n2}}{A_{+2}}\right)\left(\frac{g_{a2}}{g_{c2}}\right)\left(\frac{\lambda_{+2}}{\lambda_{n2}}\right) e^{-((E_{a1}-E_{a2}-E_{c1}+E_{c21})/kT_e)} \tag{3}$$

which is independent of the electron density n_e.

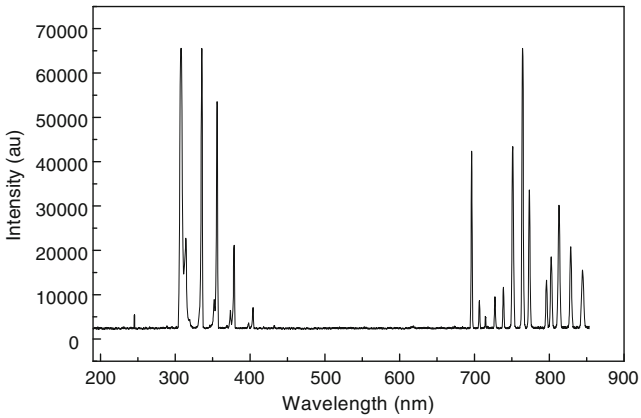

Figure 5. Optical emission lines of atmospheric pressure APGD produced in Ar.

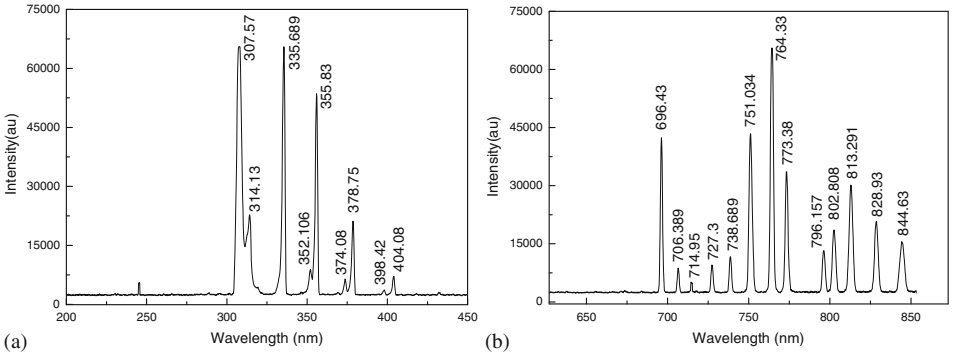

Figure 6. Ar lines obtained from the APGD in the range of 200–450 nm (**a**) and 650–850 nm (**b**).

For the four lines chosen from figure 6, the plot of $R = R_1/R_2$ against T_e is shown in figure 7. The electron temperature of the APGD has been determined to be 0.65 eV.

Using eq. (4), the electron density (n_e) can then be calculated by substituting the value of electron temperature obtained from eq. (3). Hence

$$n_e = 2 \times \frac{I_n}{I_+} \frac{\lambda_n A_+ g_+}{\lambda_+ A_n g_n} \left[\frac{2\pi m_e k T_e}{h^2}\right]^{3/2} e^{-(E_a - E_c + E_i)/kT_e}, \tag{4}$$

where I_n is the intensity of the ArI line (738.68 nm) (transition $a \rightarrow b$), I_+ is the intensity of the ArII line (398.42 nm) (transition $c \rightarrow d$) and λ_n, λ_+, A_n and A_+ are the wavelengths and probabilities of the transition. The calculated value of electron density obtained is $n_e = 6.381 \times 10^{16}$ cm^{-3}.

The electron density of the APGD can also be estimated from the Stark broadening effect for comparison. The Stark broadening arises from the interaction of atoms with

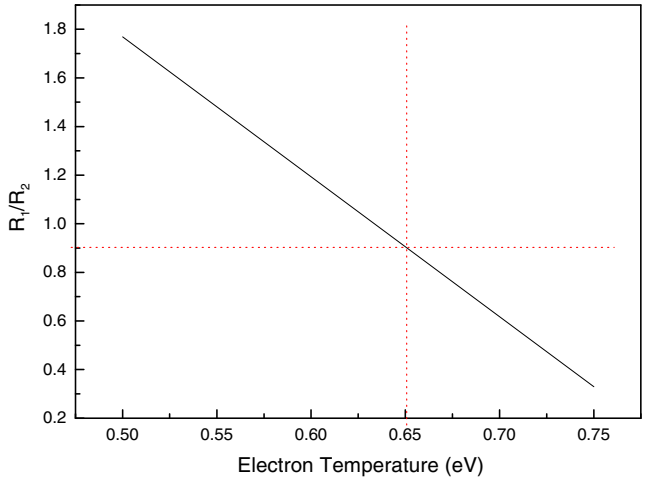

Figure 7. Plot of R_1/R_2 as a function of T_e.

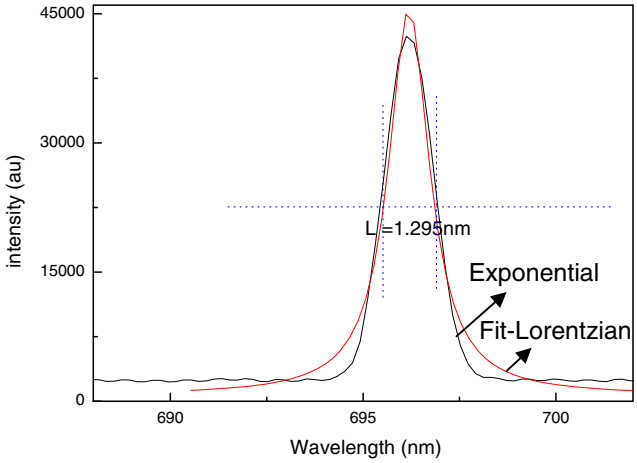

Figure 8. Recorded line profile for $\lambda_{n1} = 696.54$ nm and its Lorentzian fit.

charge particles. When electron contribution dominantes, the profile is symmetric and can be approximated by Lorentzian profile. However, asymmetries can appear when the contributions of ions become important [18] and this therefore is a limitation of the present model for determining electron density. When the electrons have dominant contribution, the expression of full-width at half-maximum (FWHM) of Stark broadening can be approximated as in (5) [19–21].

$$\Delta\lambda_{\text{Stark}} = 2 \times 10^{-11}(n_{\text{e}})^{2/3}\,. \tag{5}$$

The shape of the broadened line for $\lambda_{n1} = 696.54$ nm is Lorentzian as shown in figure 8.

The calculated value of electron density is $n_{\text{e}} = 6.04 \times 10^{16}$ cm^{-3} which agrees reasonably well with the value obtained from the line intensity ratio method.

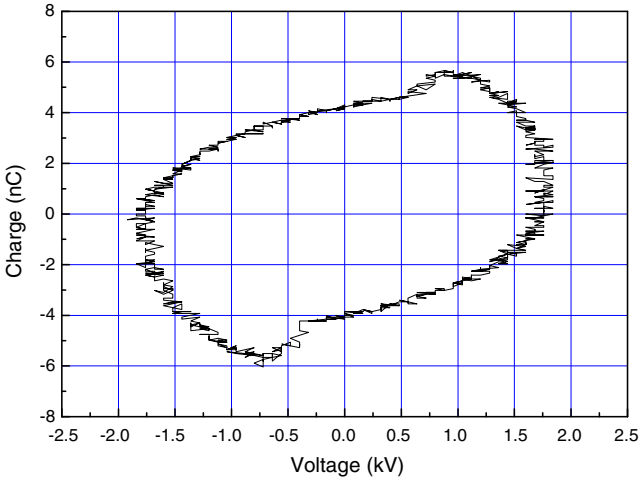

Figure 9. Lissajous figure of APGD with an electrode spacing of 0.5 mm.

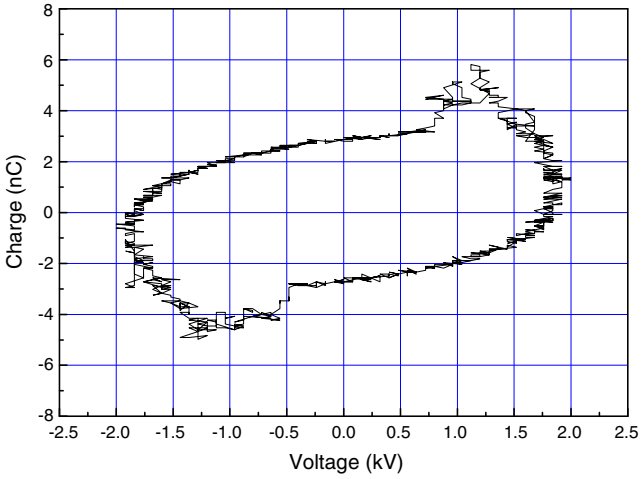

Figure 10. Lissajous figure of APGD with an electrode spacing of 1 mm.

3.3 *Calculation of energy deposited into the discharge*

Analysis of Lissajous figure is carried out in order to estimate the energy consumed per cycle in the discharge. The plot of the charge transferred (Q) during the discharge vs. the voltage applied (V) is used to calculate the energy injected into the gas. Figure 9 corresponds to the Lissajous figure of the discharge in Ar with the gap spacing of 0.5 mm. Figures 10 and 11 correspond to the discharges with 1 mm and 2 mm gaps respectively. The shapes of the Lissajous figures are not exactly parallelogram because of the difference in 'on time' and 'off time' of discharge.

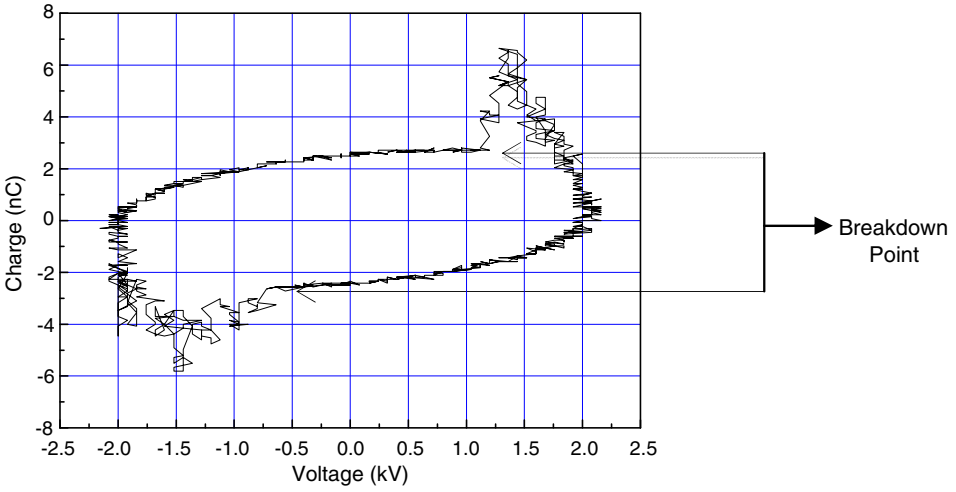

Figure 11. Lissajous figure of APGD with an electrode spacing of 2 mm. Arrows show the points when breakdown occur.

Table 1. The calculated and measured values of the energy deposited to the discharge.

Electrode gap (mm)	Calculated (μJ)	Measured (μJ)
0.5	33.4	25
1	32.3	21
2	31.5	20

A barrier discharge can be considered to be a series combination of two capacitors, one for the dielectric C_d and the other for the gas C_g. When the breakdown occurs, a resistive channel appears parallel to C_g and the charges transferred by the plasma filaments increase abruptly [22]. As long as the plasma is in ON state, the discharge current I leads the sinusoidal voltage V. The charge Q transferred by glow discharge is obtained by integrating I. For a complete cycle, the area of the Lissajous figure is proportional to the power injected into the gas. The energy deposition to the discharge, W_{dep}, is calculated as

$$W_{dep} = \frac{\langle P_{dis} \rangle}{2f}, \tag{6}$$

where P_{dis} is the average power consumed by the discharge and f is the frequency of the applied source.

By using eq. (6), the calculated values of energy deposition by discharge in 0.5 mm, 1 mm and 2 mm are summarized in table 1. The measured values of energy deposition by discharge in different gaps were estimated by measuring the area of Lissajous figures.

3.4 *Polymer surface treatment*

Atmospheric pressure plasmas in DBD and APGD modes have been widely used for polymer surface modification [23–25]. In both cases, the treatment increases the hydrophilicity of polymers. The discharge described in this paper is found to be efficient for the treatment of low-density polyethylene film. An increase in hydrophilicity of the sample is evident from figure 12. The contact angle of water drop on untreated sample is 90° and after 6 s of exposure in the discharge the contact angle decreases to 45.5°. Figure 13

(a) (b)

Figure 12. Images of sessile water drops on (**a**) untreated and (**b**) plasma-treated PE samples.

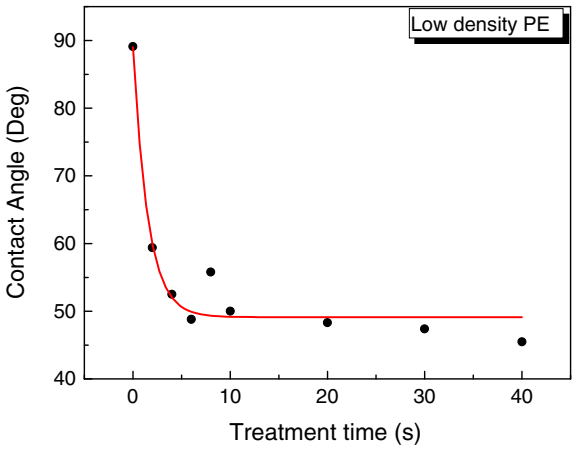

Figure 13. Contact angle of water as a function of treatment time in the discharge.

shows the change in contact angle as a function of treatment time in the discharge reaching a saturation at 6 s. This effect of treatment time on the contact angle on plasma-treated polymer is in agreement with our earlier work [25].

The decrease in contact angle can be attributed to the increase in surface roughness and incorporation of hydrophilic functional groups. This effect is obviously time-dependent as observed in our result. The appearance of saturation in the contact angles beyond a certain treatment time may be due to the establishment of equilibrium between the formation of hydrophilic functional groups on the polymer surface and their removal by etching and sputtering.

4. Conclusion

The experimental results presented in this paper showed that relatively homogeneous and non-thermal plasma could be generated at atmospheric pressure in the presence of Ar using high voltage power supply operating with a frequency in the range of a few kHz and a gap of 0.5–2 mm. Although plasma diagnostics under such condition of discharge is complicated, an attempt has been made to estimate the electron density of the discharge using both Stark broadening and line intensity ratio methods, and energy deposition could be estimated by Lissajous figure. A reasonably accurate value of electron temperature was obtained from the analysis of the optical emission spectra of the discharge. Results of contact angle measurement showed that the discharge is efficient in the surface modification of polymers.

Acknowledgement

This work was supported by the University Grants Commission (UGC), Sanothimi, Bhaktapur, Nepal.

References

[1] U Kogleschatz *et al*, *Plasma Chem. Plasma Process.* **23**, 01 (2003)
[2] A F Miralai, E Montee, R Bartnikas, G Czeremuszkin, M Latreche and M R Wertheimer, *Plasma and Polymer* **5**, 63 (2000)
[3] M Yousfi, A Bekstein, N Merbahi, O Eichwald, O Ducasse, M Benhenni and J P Gardou, *Plasma Sources Sci. Technol.* **19**, 034004 (2010)
[4] I Topala, M Asandulesh, N Dumitrascu, G Popa and J Durand, *J. Optoelectron. Adv. Mater.* **10**, 2028 (2008)
[5] S A Hashim, C S Wong, M R Abas and K Z Dahlan, *Sains Malaysiana* **39**, 981 (2010)
[6] D P Subedi, R B Tyata, A Khadgi and C S Wong, *J. Sci. Technol. Tropics* **5**, 117 (2009)
[7] T Nozaki and K Okazaki, *Pure Appl. Chem.* **78**, 1157 (2006)
[8] S Okazaki, M Kogoma, M Uehara and Y Kimura, *J. Phys. D: Appl. Phys.* **26**, 889 (1993)
[9] J Topper, M Lindmayer and B Juttner, *XIII International Conf. on Gas Discharge and their Application* (Glasgow, Scotland, 2000) Vol. 3, p. 8
[10] F Massines, A Rabehi, P Decomps, R B Gadi, P Segur and C Mayoux, *J. Appl. Phys.* **83**, 2950 (1998)
[11] J Park, I Henins, H W Hermann, G S Selwyn, J Y Jeong, R F Hicks, D Shim and C S Chang, *Appl. Phys. Lett.* **76**, 288 (2000)
[12] A A Garamoon and D M El-zeer, *Plasma Sources Sci. Technol.* **18**, 045006 (2009)
[13] S Kanazawa, M Kogoma, T Moriwaki and S Okazai, *J. Phys. D: Appl. Phys.* **21**, 838 (1988)
[14] D Trunec, A Brablec and J Buchta, *J. Phys. D: Appl. Phys.* **34**, 1697 (2001)
[15] N Gheradi and E Gat, *HAKONE VI Contr. Papers* 118 (1998)
[16] J Tepper, M Lindmayer and J Salge, *HAKONE VI Contr. Papers* 123 (1998)
[17] H Luo, Z Liang, X Wang, Z Gaun and W Liming, *J. Phys. D: Appl. Phys.* **43**, 155201 (2010)
[18] L Dong, J Ran and Z Mao, *Appl. Phys. Lett.* **86**, 161501 (2005)
[19] N Balcon, A Aanesland and R Boswell, *IOP Publishing Ltd.* **16**, 217 (2006)
[20] A Yanguas-Gil, K Focke, J Benedikt and A Von Keudell, *J. Appl. Phys.* **101**, 103307 (2007)
[21] X Ming Zhu, W Cong Chen and Y Kang Pu, *J. Phys. D: Appl. Phys.* **41** 105212 (2008)
[22] H Khatun, A Mishra, M Kumar, U Pal, A K Sharma and P K Barhai, *Indian J. Pure Appl. Phys.* **46**, 889 (2008)
[23] J Janca, P Stahel, J Buchta, D Subedi, F Krcma and J Pryckova, *Plasmas and Polymers* **6**, 15 (2001)
[24] D P Subedi, D K Madhup, A K Laghu, U M Joshi and R B Tyata, *J. Sci. Technol. Tropics* **4**, 73 (2008)
[25] D P Subedi, D K Madhup, K Adhikari and U M Joshi, *Indian J. Pure and Appl. Phys.* **46**, 540 (2008)